REVIEW ARTICLE

Importance of proper renormalization scale-setting for QCD testing at colliders

Xing-Gang Wu[1,*], Sheng-Quan Wang[1,2,†], Stanley J. Brodsky[3,‡]

[1]*Department of Physics, Chongqing University, Chongqing 401331, China*
[2]*School of Science, Guizhou Minzu University, Guiyang 550025, China*
[3]*SLAC National Accelerator Laboratory, Stanford University, Stanford, CA 94039, USA*
*E-mail: *wuxg@cqu.edu.cn, †sqwang@cqu.edu.cn, ‡sjbth@slac.stanford.edu*

A primary problem affecting perturbative quantum chromodynamic (pQCD) analyses is the lack of a method for setting the QCD running-coupling renormalization scale such that maximally precise fixed-order predictions for physical observables are obtained. The Principle of Maximum Conformality (PMC) eliminates the ambiguities associated with the conventional renormalization scale-setting procedure, yielding predictions that are independent of the choice of renormalization scheme. The QCD coupling scales and the effective number of quark flavors are set order-by-order in the pQCD series. The PMC has a solid theoretical foundation, satisfying the standard renormalization group invariance condition and all of the self-consistency conditions derived from the renormalization group. The PMC scales at each order are obtained by shifting the arguments of the strong force coupling constant α_s to eliminate all non-conformal $\{\beta_i\}$ terms in the pQCD series. The $\{\beta_i\}$ terms are determined from renormalization group equations without ambiguity. The correct behavior of the running coupling at each order and at each phase-space point can then be obtained. The PMC reduces in the $N_C \rightarrow 0$ Abelian limit to the Gell-Mann-Low method. In this brief report, we summarize the results of our recent application of the PMC to a number of collider processes, emphasizing the generality and applicability of this approach. A discussion of hadronic Z decays shows that, by applying the PMC, one can achieve accurate predictions for the total and separate decay widths at each order without scale ambiguities. We also show that, if one employs the PMC to determine the top-quark pair forward-backward asymmetry at the next-to-next-to-leading order level, one obtains a comprehensive, self-consistent pQCD explanation for the Tevatron measurements of the asymmetry. This accounts for the "increasing-decreasing" behavior observed by the D0 collaboration for increasing $t\bar{t}$ invariant mass. At lower energies, the angular distributions of heavy quarks can be used to obtain a direct determination of the heavy quark potential. A discussion of the angular distributions of massive quarks and leptons is also presented, including the fermionic component of the two-loop corrections to the electromagnetic form factors. These results demonstrate that the application of the PMC systematically eliminates a major theoretical uncertainty for pQCD predictions, thus increasing collider sensitivity to possible new physics beyond the Standard Model.

Keywords QCD, proper renormalization scale-setting, PMC, high-energy colliders

PACS numbers 12.38.Aw, 12.38.Bx

Contents

Frontiers of Physics

1 Introduction

A primary problem affecting perturbative quantum chromodynamic (pQCD) analyses of hadronic processes, such as those studied at a τ-charm factory, is the lack of a technique for systematically setting the renormalization scales μ_r of the QCD running coupling such that precise fixed-order predictions for physical observables can be obtained. In the conventional scale-setting method, a single μ_r as the argument of the QCD running coupling is simply guessed at, and this value is then varied over an arbitrary range. This scale-setting method has inherent problems. For example, the resulting pQCD predictions are dependent on the choice of renormalization scheme, in contradiction to the principle of "renormalization scheme invariance," which states that predictions for physical observables cannot depend on a theoretical convention [1]. Moreover, the error estimate obtained by varying μ_r over an arbitrary range is unreliable, as the resulting variation in the prediction is sensitive to perturbative contributions involving the pQCD β-function only. The convergence of the series is problematic because of the presence of divergent renormalon terms. In some processes, a large "K-factor" arises, e.g., for J/ψ production at a τ-charm factory. However, one cannot determine whether the large K-factor is indeed the property of the process or a false result due to the improper choice of scale. An even greater problem is that guessing at μ_r generally yields predictions for QED observables that contradict the experimentally verified, precise predictions obtained using the standard Gell-Mann-Low (GM-L) method [2].

The Principle of Maximum Conformality (PMC) [3–8] provides a systematic means of eliminating ambiguities in the renormalization scheme and in μ_r. The PMC has a rigorous theoretical foundation, satisfying the renormalization group (RG) invariance condition [9] and all of the other self-consistency conditions derived from the RG [10]. The PMC scales at each order are obtained by shifting the arguments of the running coupling to eliminate all nonconformal $\{\beta_i\}$ terms. The resulting scales also determine the correct effective number of flavors n_f at each order. The pQCD convergence is automatically improved through elimination of the divergent renormalon series. Special cases may occur in which the $\beta = 0$ conformal

terms at low orders are large, leading to large K-factors. This indicates that an even higher-order calculation is required for a reliable pQCD prediction.

The PMC reduces to the Gell-Mann-Low (GM-L) method in the $N_c \to 0$ Abelian limit [2]. Further, the PMC provides the underlying principle for the well-known Brodsky-Lepage-Mackenzie (BLM) approach [11], extending the BLM procedure unambiguously to all orders consistent with the RG. An important example of a BLM/PMC application at next-to-leading order (NLO) level is the investigation of semihard processes based on the Balitsky-Fadin-Kuraev-Lipatov (BFKL) approach [12–15]. At NLO level, the previous BLM predictions are equivalent to the PMC results as, in both cases, one must consider the β_0 terms only, which can be unambiguously fixed[1].

The PMC has been successfully applied to a number of higher-order processes, facilitating precise pQCD tests at a range of experimental facilities, including electron-positron annihilation to hadrons [7–9]; Higgs decays to $\gamma\gamma$ [16], gg, and $b\bar{b}$ [17–18]; hadronic Z decays [19]; $\Upsilon(1S)$ leptonic decay [20]; and top-pair production at the Large Hadron Collider (LHC) and Tevatron [4, 5, 21–23]. When applied to B physics, the PMC provides a possible solution to the $B \to \pi\pi$ puzzle [24].

Measurements of the rate of Z-boson decay into hadrons can constitute an important method for determining a high-precision value for the strong coupling constant α_s at a specific μ_r. This is the central goal of GigaZ [25] and other super-Z factories [26], i.e., high-luminosity e^+e^- colliders operating at Z resonance. The contributions from the nonperturbative and power-law terms are suppressed, and the smallness of α_s leads to a rapid decrease in the higher-order corrections in the pQCD series. In fact, by applying PMC scale-setting to the available pQCD predictions up to four-loop level [27–30], one obtains optimal fixed-order predictions for the Z-boson hadronic decay rate, thus enabling a very high-precision test of the Standard Model (SM) [19].

The authors of Ref. [31] have noted that an alternative scale-setting procedure, known as the "large β_0 approximation" [32, 33], leads to incorrect next-to-next-to-leading order (NNLO) n_f^2 terms for top-pair production at hadron colliders. It should be emphasized that this analytic error is a defect of the large β_0 approximation; therefore, it does not occur when PMC scale-setting is used.

It is possible for conventional scale-setting to predict, by chance and at sufficiently high order, the correct value of a global observable such as the total cross-section σ_{Total}; however, as the same μ_r is assumed at each order

---

[1] For these BLM predictions, one must ensure that only the β_0 terms that pertain to α_s running are eliminated.

in α_s, incorrect predictions are often obtained for differential observables. In fact, as in quantum electrodynamics (QED), μ_r and the effective n_f are distinct at each order of pQCD, reflecting the different virtualities of the relevant subprocesses as a function of phase space. This constitutes the underlying reason why a single "guessed" scale cannot explain the "increasing-decreasing" behavior of A_{FB} as the $t\bar{t}$-pair mass is varied. Herein, we shall show that the PMC provides a self-consistent explanation for all of the $t\bar{t}$-pair measurements at the Tevatron.

The PMC can also be applied to problems with multiple physical scales. For example, the subprocess $q\bar{q} \to Q\bar{Q}$ near the quark threshold involves not only the subprocess scale $\hat{s} \sim 4M_Q^2$, but also the $v^2\hat{s}$ scale, which appears in the Sudakov final-state corrections [34]. Here, v is the $Q\bar{Q}$ relative velocity, which becomes very small near threshold, and Q labels the heavy-quark flavor. We must introduce two PMC scales for this process, one for the hard part and one for the Coulomb terms at the currently known order of the pQCD corrections. This is an important PMC application for processes at super τ-charm factories.

The sections of this contribution to *Frontiers of Physics* are organized as follows: In Section 2, we present general arguments concerning the scale-setting problem and introduce the $\mathcal{R}_\delta$ scheme, which provides a systematic and convenient means of identifying the nonconformal β terms in a pQCD series required for computation of the PMC scales. We review several applications so as to illustrate important features of the PMC: hadronic Z decay rates; the σ and the forward-backward asymmetry A_{FB} of top-quark pair production at the Tevatron; and the angular distributions of massive quarks and leptons close to threshold, which is directly relevant to physical studies at a super τ-charm factory. This PMC application also illustrates the approach used to manage multiscale problems. A brief summary is presented in Section 3.

2 General arguments for proper scale-setting and PMC

The scale dependence of the running coupling is controlled by the renormalization group equation (RGE), which can be used recursively to establish the perturbative pattern of β terms at each order. More explicitly, the scale-displacement relation for the running coupling at two different scales, μ_1 and μ_2, defines the following β pattern at each order

$$\alpha(\mu_2) = \alpha(\mu_1) - \beta_0 \ln\left(\frac{\mu_2^2}{\mu_1^2}\right)\alpha^2(\mu_1)$$

$$+ \left[\beta_0^2 \ln^2\left(\frac{\mu_2^2}{\mu_1^2}\right) - \beta_1 \ln\left(\frac{\mu_2^2}{\mu_1^2}\right)\right]\alpha^3(\mu_1) + \dots, \quad (1)$$

where $\alpha = \alpha_s/4\pi$. The PMC utilizes this perturbative β pattern to systematically set the scale of the running coupling at each order in a pQCD expansion; the coefficients of the resulting series thus match the coefficients of the corresponding conformal theory, with $\beta = 0$. This is the same principle used in QED, where all β terms resulting from the vacuum polarization corrections to the photon propagator are absorbed into μ_r. As in QED, the scales are physical in the sense that they reflect the virtuality of the gluon propagators at a given order, and also set the effective n_f. The resulting re-summed pQCD expression thus determines the relevant "physical" scales for any physical observable, thereby providing a solution to the μ_r-setting problem.

We have previously suggested two all-order PMC approaches that are equivalent to each other at the level of conformality; therefore, they are equally viable PMC procedures [35]. In this report, we introduce the PMC approach using the $\mathcal{R}_\delta$ scheme, which can be readily automatized. The $\mathcal{R}_\delta$ method uses the β pattern generated by the RGE and its degeneracy relations to identify the terms in the pQCD series that are associated with the QCD β function, along with those that remain in the $\beta = 0$ conformal limit. The β terms are then systematically absorbed by shifting μ_r at each order, thus yielding the PMC scheme-independent prediction.

In this approach, a dimensionally arbitrary renormalization scheme is first introduced, namely, the R_δ scheme. In this scheme, an arbitrary constant $-\delta$ is subtracted in addition to the standard subtraction $\ln 4\pi - \gamma_E$ for the $\overline{\mathrm{MS}}$-scheme. Hence, the renormalization scale is redefined by an exponential factor, $\mu_\delta = \mu_{\overline{\mathrm{MS}}} \exp(\delta/2)$. The δ subtraction thus defines an infinite set of new renormalization schemes. Using the $\mathcal{R}_\delta$ scheme, one can determine the β pattern at each perturbative order [7, 8]. The QCD prediction ϱ_n of a physical observable ϱ can be expressed as

$$\varrho_n(Q) = r_{0,0} + r_{1,0}\alpha(\mu_r) + [r_{2,0} + \beta_0 r_{2,1}]\alpha^2(\mu_r)$$
$$+ [r_{3,0} + \beta_1 r_{2,1} + 2\beta_0 r_{3,1} + \beta_0^2 r_{3,2}]\alpha^3(\mu_r) + \cdots,$$
$$(2)$$

where Q represents the scale at which ϱ is measured and the $r_{i,j}$ coefficients are functions of the initial choice of μ_r and Q. The $r_{i,0}$ are the conformal coefficients. Here, the β pattern for the pQCD series at each order is a superposition of all of the $\{\beta_i\}$ terms that govern the evolution of the lower-order α_s contributions at this particular order.

After applying the standard scale-setting procedures by setting the PMC scales Q_i, the final pQCD predic-

tion for ϱ_n reads

$$\varrho_n(Q) = r_{0,0} + \sum_{i=1}^{n} r_{i,0}\alpha^i(Q_i). \qquad (3)$$

The Q_i and $r_{i,0}$ can be found in Ref. [8], with the former being functions of μ_r and Q. The resulting Q_i values are independent of the choice of initial μ_r at infinite order, ensuring RG invariance. Thus, one can adopt any initial value of μ_r (the only requirement is that it is within the perturbative region) and obtain the same pQCD prediction. At fixed orders, a small residual scale uncertainty in Q_i can be noted and, hence, in the final pQCD expression due to the truncation of the β function; however, these residual uncertainties are found to be highly suppressed and, in fact, negligible, even for lower-order predictions. Thus, the conventional μ_r dependence has been eliminated. In practice, one can take the usual choice of μ_r, e.g., the typical momentum flow of the process, as the initial scale, so as to simplify the pQCD expressions and the PMC treatment.

The PMC eliminates the dependence on the renormalization scheme and on μ_r that characterize the conventional scale-setting methods. However, it does not violate other properties of the pQCD series, such as gauge invariance. Moreover, the PMC correctly sets μ_r at each pQCD order; thus, in distinction to conventional scale-setting, it simultaneously predicts the correct values for both σ_{Total} (or the total decay width) and the differential observables.

2.1 Higher-order pQCD corrections to hadronic Z decays

The decay rate of the Z boson into hadrons can be expressed as

$$\Gamma_Z = \mathcal{C}\left[\sum_f v_f^2 r_{NS}^V + \left(\sum_f v_f\right)^2 r_S^V + \sum_f a_f^2 r_{NS}^A + r_S^A\right],$$

where $\mathcal{C} = 3\frac{G_F M_Z^3}{24\pi\sqrt{2}}$ (where M_Z is the mass of the Z boson), $v_f \equiv 2I_f - 4q_f s_W^2$, $a_f \equiv 2I_f$, q_f is the f-quark electric charge, s_W is the effective weak mixing angle, and I_f is the third component of the weak isospin of the left-handed component of f. Further, $r_{NS}^V = r_{NS}^A \equiv r_{NS}$, r_S^V, and r_S^A represent the non-, vector-, and axial-singlet components, respectively. These contributions can be further expressed as

$$r_{NS} = 1 + \sum_{i=1}^{n} C_i^{NS} a_s^i, \quad r_S^V = \sum_{i=3}^{n} C_i^{VS} a_s^i,$$

$$r_S^A = \sum_{i=2}^{n} C_i^{AS} a_s^i,$$

where $a_s = \alpha_s/\pi$. The coefficients of r_{NS}, r_S^V, and r_S^A, with their dependence on the initial choice of scale, can be derived from Refs. [27–30]. Each physical contribution to the Z decay has a different momentum flow; thus, the PMC scales for r_{NS}, r_S^V, and r_S^A should be set individually [19]. The prediction for a physical observable should not depend on the scheme or the initial choice of scale. We shall take r_{NS} as an example to show that the computed PMC scales and, thus, the final PMC predictions for the hadronic Z decay results, are highly scale independent.

We present the scale dependence before (with conventional scale-setting) and after PMC scale-setting for r_{NS} in Fig. 1. As expected, for the conventional scale-setting, the resulting low-order predictions depend heavily on μ_r. However, one observes that a weaker scale dependence is achieved as more loops are taken into consideration, which is as expected. On the other hand, following application of the PMC, the pQCD predictions at each order are almost independent of μ_r. This is because the PMC scales at each order are determined unambiguously through absorbance of all non-conformal β terms into the running coupling. This also indicates that the PMC predictions have the property that any residual dependence on the initial choice of μ_r is highly suppressed, even for low-order predictions. Figure 1 shows not only that the μ_r ambiguities are eliminated, but also that the value of r_{NS} rapidly approaches its steady point; i.e., the curves at NLO, N²LO, and N³LO almost coincide with each other following application of the PMC.

We emphasize that, following application of the PMC, one obtains improved pQCD convergence as a result of the elimination of the renormalon terms. The pQCD estimations at each perturbative order for r_{NS} are presented in Table 1 The fastest pQCD convergence is thus achieved by applying the PMC. The pQCD correction at $\mathcal{O}(\alpha_s^4)$ is –0.000 16 for the conventional scale-setting, which leads to a shift of the central value of $\alpha_s(M_Z)$ from 0.1185 to 0.1190 [28, 29]. In contrast, after applying the PMC, this correction becomes negligible (−0.000 01). Table 1 also shows that the predictions for the total sum $\sum_{i=1}^{4} R_i^{NS}$ for both PMC and conventional scale-setting are close in value, although their perturbative series behave very differently.

Table 1 Perturbative contributions for the non-singlet r_{NS} under the conventional (Conv.) and the PMC scale settings. Here, $R_i^{NS} = C_i^{NS} a_s^i$ with $i = (1, \cdots, 4)$ stand for the one-, two-, three-, and four-loop terms, respectively. $\mu_r = M_Z$.

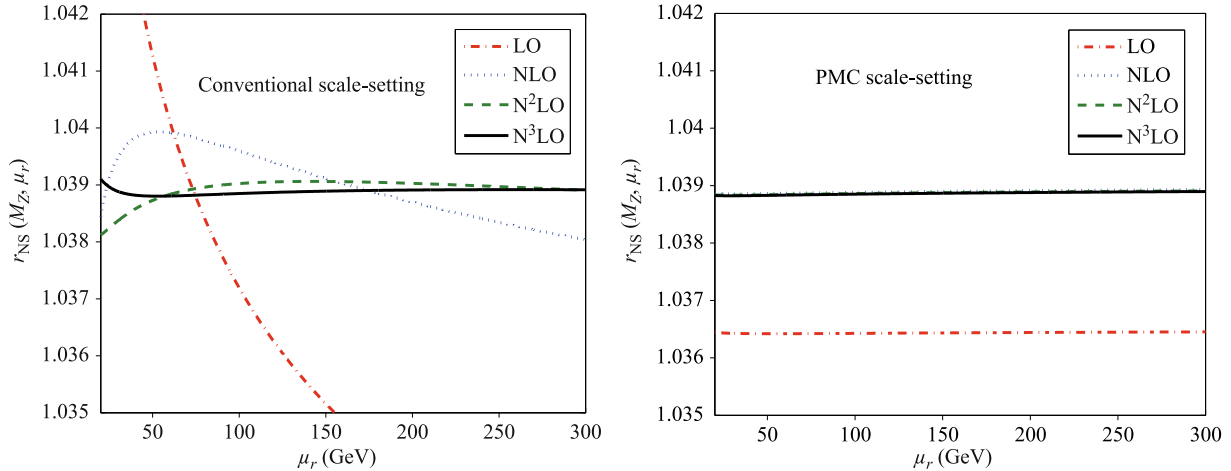|	R_1^{NS}	R_2^{NS}	R_3^{NS}	R_4^{NS}	$\sum_{i=1}^{4} R_i^{NS}$
Conv.	0.03769	0.00200	−0.00069	−0.00016	0.03884
PMC	0.03636	0.00252	−0.00003	−0.00001	0.03885

Fig. 1 The non-singlet contribution r_{NS} up to four-loop QCD corrections versus μ_r before and after PMC scale-setting. After PMC scale-setting, the curves for NLO, N^{2}LO, and N^{3}LO are almost coincide with each other.
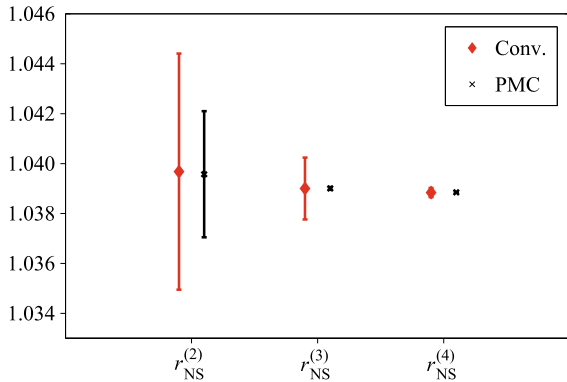

Fig. 2 The values of $r_{NS}^{(n)} = 1 + \sum_{i=1}^{n} C_i^{NS} a_s^i$ and their errors $\pm|C_n^{NS} a_s^n|_{MAX}$. The diamonds and the crosses are for conventional (Conv.) and PMC scale settings, respectively. The central values assume the initial scale choice $\mu_r = M_Z$.

The ability to estimate the magnitudes of the "unknown" higher-order pQCD corrections is helpful. One typically estimates those unknown contributions by varying $\mu_r \in [M_Z/2, 2M_Z]$. However, this simple procedure only exposes the β-dependent non-conformal terms, rather than the entire perturbative series. We emphasize that the scales are optimized and cannot be varied following application of the PMC; otherwise, the RG invariance would be explicitly violated, leading to an unreliable prediction. Here, for a conservative estimate, we take the uncertainty to be the last-known perturbative order [9]; i.e., at n-th order, the perturbative uncertainty is estimated using $\pm|C_n^{NS} a_s^n|_{MAX}$ (where "MAX" indicates the maximum of $|C_n^{NS} a_s^n|$) by varying μ_r within the $[M_Z/2, 2M_Z]$ region. The error bars for the PMC and the conventional scale-setting are displayed in Fig. 2. It can be seen that the predicted error bars from the "unknown" higher-order corrections quickly approach their steady points following application of the PMC. These error bars pro-

vide a consistent estimate of the "unknown" QCD corrections under conventional and PMC scale-settings; i.e., the exact value for "unknown" $r_{NS}^{(n)}$ ($n = 3$ and 4) is well within the error bars predicted from $r_{NS}^{(n-1)}$.

2.2 Yields and forward-backward asymmetry of top-pair productions at the tevatron

In the following, we summarize our recent results for the yields and A_{FB} of top-pair productions at the Tevatron, for a hadron-hadron collision energy of $\sqrt{S} = 1.96$ TeV.

2.2.1 Production cross-section of $t\bar{t}$

The NNLO total cross-sections from all the production channels, i.e., the $q\bar{q}$, gq, $g\bar{q}$, and gg channels, before (with conventional scale-setting) and after PMC scale-setting, are [23]

$$\sigma_{Total}|_{Conv.} = 7.42^{+0.25}_{-0.29} \text{ pb}, \tag{4}$$

$$\sigma_{Total}|_{PMC} \simeq 7.55 \text{ pb}, \tag{5}$$

for conventional ("Conv.") and PMC scale-setting, respectively, where the errors are obtained by varying the initial $\mu_r \in [m_t/2, 2m_t]$. $\sigma_{Total}|_{PMC}$ is almost unchanged from $\sigma_{Total}|_{Conv.}$, indicating that the residual scale dependence is negligible. Both the PMC and conventional scale-setting procedures agree with the Collider Detector at Fermilab (CDF) and D0 collaboration measurements within the accepted error range; the recent combined cross-section given by the CDF and D0 collaborations is 7.60 ± 0.41 pb [36]. The dependence of σ_{Total} on the choice of μ_r is also small when conventional scale-setting is used, provided NNLO QCD corrections are incorporated.

Frontiers of Physics

Table 2 The $(q\bar{q})$-channel cross-sections (in unit: pb) at each perturbative order under the conventional and PMC scale-settings [23], where three typical renormalization scales, $\mu_r = m_t/2$, m_t and $2m_t$, are adopted. The factorization scale is taken as $\mu_f = m_t$.

μ_r	Conventional			PMC
	$m_t/2$	m_t	$2m_t$	$[m_t/2, 2m_t]$
$\sigma_{q\bar{q}}^{\mathrm{LO}}$	5.99	4.90	4.09	$\simeq 4.76$
$\sigma_{q\bar{q}}^{\mathrm{NLO}}$	0.09	0.96	1.41	$\simeq 1.73$
$\sigma_{q\bar{q}}^{\mathrm{N^2LO}}$	0.45	0.48	0.63	$\simeq -0.06$

Eq. (4) shows that, for conventional scale-setting, the σ_{Total} scale dependence at the NNLO level is small; i.e., the scale error is $\left(^{+3\%}_{-4\%}\right)$. However, the use of a single guessed scale does not yield correct predictions of the cross-sections for individual channels at each order. In fact, through detailed analysis of the pQCD series, we find that the errors for the separate cross-sections at each order for conventional scale-setting are large in all of the contributing channels. As an example, the contributions of the dominant $q\bar{q}$ channel both with and without PMC scale-setting are presented in Table 2. To show the scale dependence of the individual cross-sections $\sigma_{q\bar{q}}^i$, we define a ratio κ_i such that

$$\kappa_i = \frac{\sigma_{q\bar{q}}^i\big|_{\mu_r=m_t/2} - \sigma_{q\bar{q}}^i\big|_{\mu_r=2m_t}}{\sigma_{q\bar{q}}^i\big|_{\mu_r=m_t}},$$

where i=LO, NLO, and N^{2}LO, respectively. Using conventional scale-setting, we obtain

$$\kappa_{\mathrm{LO}} = 39\%, \ \kappa_{\mathrm{NLO}} = -138\%, \ \kappa_{\mathrm{N^2LO}} = -36\%.$$

These results show that the dependence on the initial choice of scale at each order is very large for conventional scale-setting. For example, the scale dependence of the NLO cross-section $\sigma_{q\bar{q}}^{\mathrm{NLO}}$, which gives the dominant component of A_{FB}, can be up to -138%. On the other hand, for the PMC, all of the κ_i values are less than 0.1%; this indicates the scale dependence of each loop term is eliminated simultaneously.

In these calculations, we set the factorization scale μ_f to μ_r. The determination of μ_f is a completely separate issue from the setting of μ_r, as it is present even for a conformal theory with $\beta = 0$. The value of μ_f should be chosen to match the nonpertubative bound-state dynamics with perturbative Dokshitzer-Gribov-Lipatov-Altarelli-Parisi (DGLAP) evolution, which can be achieved explicitly using nonperturbative models such as anti-de Sitter (AdS)/QCD and light-front holography, where the light-front wavefunctions of the hadrons are known. (See the recent review [37].) We have found that the μ_f dependence is decreased following application of the PMC [22]. In contrast, the simple conventional scale-setting proce-

dure, in which $\mu_r = m_t$ is selected in order to eliminate the log terms $\ln^k \mu_r^2/m_t^2$, is again problematic, as it may lead to a large μ_f dependence. This again confirms the importance of proper μ_r setting.

2.2.2 Forward-backward asymmetry of $t\bar{t}$

The top-quark pair A_{FB} in $\bar{p}p \rightarrow t\bar{t}X$ collisions is also sensitive to the μ_r-setting procedure. This asymmetry is dominated by interference between different amplitudes contributing to the $q\bar{q}$ channel. Contributions to A_{FB} begin at the NLO level. Thus, evaluating the correct value for the NLO terms is very important in order to achieve an accurate prediction for the $t\bar{t}$ A_{FB}. However, the accuracy of the value of $\sigma_{q\bar{q}}^{\mathrm{NLO}}$ derived using conventional scale-setting is questionable, because of the associated large scale errors, i.e., $\kappa_{\mathrm{NLO}} \sim -138\%$. Moreover, if one uses conventional scale-setting, $\sigma_{q\bar{q}}^{\mathrm{NLO}}$ increases and the total cross-section $\sigma_{q\bar{q}}^{\mathrm{Total}}$ decreases as μ_r is increased. Thus, in order to obtain agreement with the measured $\sigma_{q\bar{q}}^{\mathrm{Total}}$, the conventional method requires a smaller $\mu_r = m_t/2$. However, this leads to the prediction of a small $t\bar{t}$ A_{FB}, which is well below the values obtained from experimental data. This example shows why previous NLO SM predictions could not yield a consistent simultaneous explanation of both the top-pair $\sigma_{q\bar{q}}^{\mathrm{Total}}$ and the $t\bar{t}$ A_{FB}.

It is important to note the NLO PMC scale $\mu_r^{\mathrm{PMC,NLO}}$ of the $q\bar{q}$ channel is significantly smaller than m_t. It is dominated by the non-Coulomb n_f terms at the α_s^4 order, which are shown in Fig. 3. In these diagrams, the momentum flow of the virtual gluons has a large range of virtualities. The NLO PMC scale is numerically small, as it is, in effect, a weighted average of the different gluon momentum flows. The resulting $\sigma_{q\bar{q}}^{\mathrm{NLO}}$ is, in fact, approximately twice as large as the cross-section predicted by conventional scale-setting; the precision of the predicted A_{FB} is also greatly improved.

Moreover, as shown in Table 2, following application of the PMC, the predicted ratio of the cross-section at the N^{2}LO level for the $q\bar{q}$ channel to $\sigma_{q\bar{q}}^{\mathrm{NLO}}$, i.e., $|\sigma_{q\bar{q}}^{\mathrm{N^2LO}}/\sigma_{q\bar{q}}^{\mathrm{NLO}}|$, is reduced from $\sim 50\%$ to less than $\sim 4\%$. This shows that a considerable improvement in pQCD
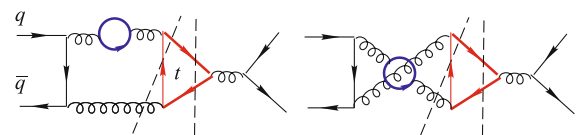

Fig. 3 Dominant cut diagrams for the n_f-terms at the α_s^4-order of the $(q\bar{q})$-channel, which are responsible for the smaller effective NLO PMC scale, where the solid circles stand for the light quark loops.

convergence can be achieved using the PMC. Such an improvement in the pQCD convergence is essential to achieve accurate pQCD predictions for the $t\bar{t}$ $A_{\rm FB}$. If we further include the $\mathcal{O}(\alpha_s^2\alpha)$ and $\mathcal{O}(\alpha^2)$ electroweak contributions, we achieve a precise SM "NLO asymmetry" prediction [21]

$$A_{\rm FB}^{\rm PMC} = \frac{\alpha_s^3 N_1 + \alpha_s^2 \alpha \tilde{N}_1 + \alpha^2 \tilde{N}_0}{\alpha_s^2 D_0 + \alpha_s^3 D_1}, \qquad (6)$$

where the D_i and N_i terms represent the total cross-sections at each α_s order and the corresponding asymmetric contributions, respectively. The $\tilde{N}_1$ term corresponds to the QCD-QED interference contribution at $\mathcal{O}(\alpha_s^2\alpha)$ order, and $\tilde{N}_0$ is the pure electroweak antisymmetric $\mathcal{O}(\alpha^2)$ contribution arising from $|\mathcal{M}_{q\bar{q}\to\gamma\to t\bar{t}} + \mathcal{M}_{q\bar{q}\to Z^0\to t\bar{t}}|^2$. From Eq. (6), we obtain a precise prediction for $A_{\rm FB}$ with no renormalization scale uncertainty [23], i.e., $A_{\rm FB}^{\rm PMC} = 9.2\%$, which agrees with D0 measurements within the acceptable error range, $A_{\rm FB}^{\rm D0} = (10.6 \pm 3.0)\%$ [38] and $A_{\rm FB}^{\rm D0} = (11.8 \pm 2.5 \pm 1.3)\%$ [39].

We can also use the PMC to predict the top-quark pair $A_{\rm FB}(M_{t\bar{t}} > M_{\rm cut})$ as a function of the top-pair invariant mass lower limit $M_{\rm cut}$ ($M_{t\bar{t}}$ is the mass of the top-quark pair). In the case of $M_{\rm cut} = 450$ GeV, the $A_{\rm FB}$ predicted using conventional scale-setting is $A_{\rm FB}(M_{t\bar{t}} > 450 \text{ GeV})|_{\rm Conv.} = 12.9\%$. This becomes even larger following application of the PMC, i.e., $A_{\rm FB}(M_{t\bar{t}} > 450 \text{ GeV})|_{\rm PMC} = 29.9\%$. The prediction using conventional scale-setting deviates significantly from the CDF measurements $(47.5 \pm 11.4)\%$ [40] and $(29.5 \pm 5.8 \pm 3.3)\%$ [41]. In contrast, the PMC prediction agrees with the weighted average of the CDF measurements [40, 41] within the accepted error. Thus, following application of the PMC, the large discrepancies between the SM estimates and the CDF measurements obtained using conventional scale-setting are removed.

The most recent measurements reported by the D0

collaboration [38] indicate a non-monotonic, increasing-decreasing behavior for $A_{\rm FB}(M_{t\bar{t}} > M_{\rm cut})$ as the lower limit of the $t\bar{t}$ mass is increased. This behavior cannot even be explained by a NNLO QCD calculation using conventional scale-setting, which predicts monotonically increasing behavior [31]. More explicitly, if conventional scale-setting using a fixed scale of m_t is employed, then $A_{\rm FB}(M_{t\bar{t}} > M_{\rm cut})$ monotonically increases with increasing $M_{\rm cut}$, as shown in Table 3. In contrast, under application of the PMC, $A_{\rm FB}(M_{t\bar{t}} > M_{\rm cut})$ first increases and then decreases as the lower limit of the pair mass $M_{\rm cut}$ is increased. These trends are more clearly shown in Fig. 4, in which the SM predictions using conventional and PMC scale-settings are compared with CDF [41] and D0 [38] measurements. The PMC predictions can be understood in terms of the behavior of the effective pQCD coupling $\bar{\alpha}_s(\overline{\mu}_r^{\rm PMC})$; this is the weighted average of the running couplings entering the $q\bar{q}$ channel, which is the subprocess underlying the asymmetry in pQCD. Note that $\bar{\alpha}_s(\overline{\mu}_r^{\rm PMC})$ has a detailed dependence on the kinematics, and the non-monotonic behavior of the effective coupling accounts for the "increasing-decreasing" behavior of $A_{\rm FB}(M_{t\bar{t}} > M_{\rm cut})$ [23]. We have also recently shown [22] that the PMC predictions are in agreement with the available A Toroidal LHC Apparatus (ATLAS) and Compact Muon Solenoid (CMS) data. Thus, the proper setting of the renormalization scale provides a consistent SM explanation of the top-quark pair $A_{\rm FB}$ measurements at both the Tevatron and LHC.

Table 3 Top-quark pair asymmetries $A_{\rm FB}(M_{t\bar{t}} > M_{\rm cut})$ using conventional (Conv.) and PMC scale-setting procedures [23], respectively. The predictions are shown for typical values of $M_{\rm cut}$. The initial scale $\mu_r = m_t$.

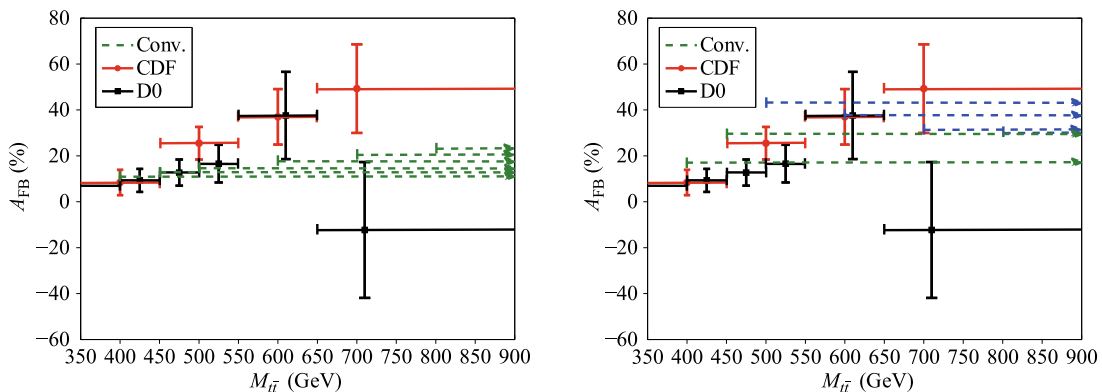| $A_{\rm FB}(M_{t\bar{t}} > M_{\rm cut})$	$M_{\rm cut}$ (GeV)					
	400	450	500	600	700	800
Conv.	11%	13%	15%	18%	21%	23%
PMC	17%	30%	44%	38%	31%	30%

Fig. 4 A comparison of SM predictions of $A_{\rm FB}$ using conventional (Conv.) and PMC scale-settings with the CDF [41] and D0 [38] measurements [23]. The initial scale $\mu_r = m_t$.

2.3 Angular distributions of massive quarks and leptons close to threshold

The PMC can also be applied to problems with multiple physical scales. The $t\bar{t}$-pair hadronic production examined at the Tevatron and LHC has already provided one such example. For the hard part at the two-loop level, we must introduce two PMC scales. The Coulomb-type corrections in the threshold region are enhanced by factors of π; thus, the terms that are proportional to (π/v) or $(\pi/v)^2$ must be treated separately and an extra PMC scale that is relatively soft for $v \to 0$ must be introduced [4]. As another example, note that a BLM analysis of the angular distributions of massive quarks and leptons close to threshold has been conducted. This study has shown that the subprocess $q\bar{q} \to Q\bar{Q}$ near the quark threshold involves not only the subprocess scale $\sqrt{\hat{s}} \sim 2M_Q$, but also the $v\sqrt{\hat{s}}$ scale, which enters the Sudakov final-state corrections [34]. At this order, the BLM and PMC predictions are identical. Therefore, for this particular process, we can treat the BLM and PMC as being on an equal footing. More explicitly, we must introduce two PMC scales for this process, one for the hard part and one for the Coulomb-type terms. This example also illustrates the approach to multi-scale problems, which is relevant for processes that can be studied at a super τ-charm factory or high-intensity electro-proton accelerators with similar center-of-mass collision energy.

An important consequence of the heavy-quark kinematics is that the production angle of a heavy hadron follows the direction of the parent heavy quark. Close to threshold at the $v \to 0$ limit, the center-of-mass angular distribution for $e^+e^- \to Q\bar{Q}$ is isotropic as a result of S-wave dominance. The small admixture of P waves slightly above threshold provides a contribution that is proportional to $v^2 \cos\theta$. The angular distribution is measurable, and one can define the "anisotropy" $A(v^2)$ of the process as

$$\frac{\mathrm{d}N}{\mathrm{d}\cos\theta} \propto 1 + A(v^2)\cos^2\theta. \tag{7}$$

Further, $A(v^2)$ can determined by the Dirac F_1 and Pauli F_2 form factors via [34]

$$A = \frac{\tilde{A}}{1 - \tilde{A}}, \tag{8}$$

with

$$\tilde{A} = \frac{v^2}{2}\frac{|F_1|^2(1-\beta^2) - |F_2|^2}{|F_1 + F_2|^2(1-\beta^2)}. \tag{9}$$

The two-loop-QED corrections to $F_{1,2}$ have been calculated in Ref. [43]; thus, one can set their renormalization scales by applying the PMC. For example, we obtain [34]

$$F_1 + F_2 = 1 + \frac{\pi\alpha(v\sqrt{\hat{s}})}{4v} - 2\frac{\alpha(\sqrt{\hat{s}}e^{3/8}/2)}{\pi} \tag{10}$$

$$\simeq \left[1 - 2\frac{\alpha(\sqrt{\hat{s}}e^{3/8}/2)}{\pi}\right]\left[1 + \frac{\pi\alpha(\sqrt{\hat{s}}v)}{4v}\right]. \tag{11}$$

Two distinctly different correction factors are obtained: The first originates from hard transverse photon exchange, where the scale reflects the short distance process; the second arises from the instantaneous Coulomb potential. All of the $1/v$ terms can then be re-summed using Sommerfeld's re-scattering formula. For example, from Eq. (11) we can obtain

$$|F_1 + F_2|^2 \simeq \left[1 - 4\frac{\alpha(\sqrt{\hat{s}}e^{3/8}/2)}{\pi}\right]\frac{x}{1 - e^{-x}}, \tag{12}$$

where $x = \pi\alpha(\sqrt{\hat{s}}v)/v$. One can take $\hat{s} \simeq 4m_Q^2$ in the threshold region. In this manner, $|F_1|^2$, $|F_2|^2$, and $|F_1 + F_2|^2$ can be predicted and, thus, accurate predictions of A can be made. These formulae can be conveniently matched to the QCD case using the effective charge of the potential α_V [34]. Because A is sensitive to $\alpha_V(\sqrt{\hat{s}}v)$, the measurement of this property can provide a check on other determinations of α_V.

The anisotropy of τ pairs produced through the $e^+e^- \to \tau^+\tau^-$ channel can also be used in an analogous manner to measure the Pauli form factor of the τ lepton $F_2(\hat{s})$ in the threshold domain $\hat{s} \geqslant 4m_\tau^2$. Thus, a precise measurement of A could provide a novel measurement of a fundamental parameter of the τ lepton and its time-like anomalous magnetic moment.

3 Summary

It is clearly important and fundamental to set the renormalization scale in a manner consistent with the principles of the renormalization group. The most critical criterion is that a prediction for a physical observable cannot depend on a theoretical convention, such as the choice of renormalization scheme or (initial) scale. This principle is satisfied by Gell–Mann–Low scale-setting, which is rigorously used for precision quantum electrodynamic (QED) predictions. The QED scale is unambiguous, and the resulting high-precision predictions are identical in any scheme and at any finite order. The same properties are also satisfied for non-Abelian gauge theory when principle-of-maximum-conformality (PMC) scale-setting is employed. The PMC can be applied to any high-order process, thus facilitating precise tests of theory at any experimental facility.

We have illustrated the main features of PMC predictions for hadronic Z decays, the yields and the forward-backward asymmetry of the top-quark pair at the Tevatron, and the production of massive quarks and leptons close to threshold. In contrast to predictions obtained using conventional scale-setting, one finds the following for the PMC:

- All terms in the perturbative quantum chromodynamic (pQCD) series involving the β function are absorbed into the running coupling order-by-order. The value of the PMC scale at each order is fixed, which also determines the effective number of contributing flavors at each order, as in QED. One finds that the PMC predictions exhibit negligible initial scale independence for both the global and differential observables at each order and phase-space point. Small initial scale dependence can also often be achieved using conventional scale-setting at very high orders in pQCD; however, this is typically the result of cancellation among different orders or phase-space points. Nevertheless, the scale dependences for differential observables at each order can remain very large. This fact underlies the inconsistency between conventional predictions of the top-quark pair asymmetry and measured values.

  When the PMC is employed, a large $t\bar{t}$ asymmetry is predicted, in agreement with experimental data. This can be traced to the fact that a smaller effective PMC scale controls the next-to-leading order (NLO) terms of the $q\bar{q}$ channel, resulting in an enhanced NLO contribution. Furthermore, the next-to-next-to-leading order (NNLO) terms are negligible as a result of the improved pQCD convergence. The effective scale is determined by a NNLO β_0 term that is independent of the choice of initial scale; its behavior versus $M_{t\bar{t}}$ explains the "increasing-decreasing" behavior measured by the D0 collaboration. The NNLO calculation of the top-pair asymmetry using conventional scale-setting can also predict a reasonably large top-pair asymmetry. This is, however, due to a large contribution at NNLO. The conventional technique exhibits a large scale uncertainty, and it cannot explain the observed "increasing-decreasing" behavior as a function of the $t\bar{t}$ invariant mass.

- Only those β terms that pertain to the running of α_s should be eliminated. One can confirm that the nonconformal β terms are correctly identified and absorbed by the PMC procedure by checking that the fixed-order theory prediction exhibits negligible

dependence on the choice of initial scale. Some dependence on the initial scale can persist when the PMC is employed, which is due to unknown higher-order terms; however, this dependence is highly suppressed even for low-order predictions.

- The resulting coefficients of the pQCD series at any perturbative order using the PMC method are, thus, identical to those of the corresponding conformal theory with $\beta = 0$, and the PMC predictions are, therefore, scheme independent. Such scheme independence is exact for all dimensional-like $\mathcal{R}_\delta$ schemes [7, 8]. One can also obtain scheme-independent predictions for effective charges using "commensurate scale relations" [42]. In principle, some residual scheme dependence may occur if a non-dimensional regularization scheme is used; this is due to unknown higher-order β terms. In such a case, the PMC scale for the highest-known terms can only be determined by one-order-higher terms, which may be unknown. Thus, one cannot obtain a complete commensurate scale relation at this particular order. However, as a result of the elimination of the divergent renormalon terms, the value of the highest-known term itself is usually small; therefore, such residual scheme dependence is typically highly suppressed.

- PMC scale-setting can also be systematically applied to multi-scale problems. The typical momentum flow can be distinct; thus, one should apply the PMC separately in each region. For example, two PMC scales arise at NNLO for the production of massive quarks and leptons close to threshold [34], with one being proportional to $\sqrt{\hat{s}}$ and the other to $v\sqrt{\hat{s}}$ (v is the $Q\bar{Q}$ relative velocity).

  Cases exist in which additional momentum flows occur, again contradicting conventional scale-setting; however, the PMC eliminates such ambiguities. For example, there are two types of log terms, $\ln(\mu_r/M_Z)$ and $\ln(\mu_r/M_t)$, for the axial singlet r_S^A of hadronic Z decays (μ_r, M_Z, and M_t are the renormalization scale and the masses of the Z boson and top quark, respectively). By applying the PMC, one finds the scale is $Q^{\rm AS} \simeq 100$ GeV [19], indicating that the typical momentum flow for r_S^A is closer to M_Z than M_t.

The PMC is an important theoretical tool that facilitates precise, reliable predictions for QCD. The PMC rigorously eliminates the usual ambiguities associated with the renormalization scale-setting procedure, yielding predictions that are independent of the choice of renormal-

ization scheme. The QCD coupling scales and the effective number of quark flavors are systematically set, order-by-order, even for multi-scale applications. The usual $n!$ divergent renormalon behavior of the perturbative expansion is also eliminated.

The application of the PMC can thus greatly improve the precision of QCD tests at super τ-charm factories and the sensitivity of measurements conducted at the LHC and other colliders to new physics beyond the Standard Model.

References

1. X. G. Wu, S. J. Brodsky, and M. Mojaza, The renormalization scale-setting problem in QCD, *Prog. Part. Nucl. Phys.* 72, 44 (2013)

2. M. Gell-Mann and F. E. Low, Quantum electrodynamics at small distances, *Phys. Rev.* 95, 1300 (1954)

3. S. J. Brodsky and X. G. Wu, Scale setting using the extended renormalization group and the principle of maximum conformality: The QCD coupling constant at four loops, *Phys. Rev. D* 85, 034038 (2012) [*Phys. Rev. D* 86, 079903 (2012)]

4. S. J. Brodsky and X. G. Wu, Application of the principle of maximum conformality to top-pair production, *Phys. Rev. D* 86, 014021 (2012) [*Phys. Rev. D* 87, 099902 (2013)]

5. S. J. Brodsky and X. G. Wu, Eliminating the renormalization scale ambiguity for top-pair production using the principle of maximum conformality, *Phys. Rev. Lett.* 109, 042002 (2012)

6. S. J. Brodsky and L. Di Giustino, Setting the renormalization scale in QCD: The principle of maximum conformality, *Phys. Rev. D* 86, 085026 (2012)

7. M. Mojaza, S. J. Brodsky, and X. G. Wu, Systematic all-orders method to eliminate renormalization-scale and scheme ambiguities in perturbative QCD, *Phys. Rev. Lett.* 110, 192001 (2013)

8. S. J. Brodsky, M. Mojaza, and X. G. Wu, Systematic scale-setting to all orders: The principle of maximum conformality and commensurate scale relations, *Phys. Rev. D* 89, 014027 (2014)

9. X. G. Wu, Y. Ma, S. Q. Wang, H. B. Fu, H. H. Ma, S. J. Brodsky, and M. Mojaza, Renormalization group invariance and optimal QCD renormalization scale-setting, arXiv: 1405.3196 [hep-ph]

10. S. J. Brodsky and X. G. Wu, Self-consistency requirements of the renormalization group for setting the renormalization scale, *Phys. Rev. D* 86, 054018 (2012)

11. S. J. Brodsky, G. P. Lepage, and P. B. Mackenzie, On the elimination of scale ambiguities in perturbative quantum chromodynamics, *Phys. Rev. D* 28, 228 (1983)

12. S. J. Brodsky, V. S. Fadin, V. T. Kim, L. N. Lipatov, and G. B. Pivovarov, The QCD pomeron with optimal renormalization, *JETP Lett.* 70, 155 (1999)

13. M. Hentschinski, A. Sabio Vera, and C. Salas, Hard to soft pomeron transition in small-x deep inelastic scattering data using optimal renormalization, *Phys. Rev. Lett.* 110, 041601 (2013)

14. X. C. Zheng, X. G. Wu, S. Q. Wang, J. M. Shen, and Q. L. Zhang, Reanalysis of the BFKL Pomeron at the next-to-leading logarithmic accuracy, *J. High Energy Phys.* 1310, 117 (2013)

15. F. Caporale, D. Y. Ivanov, B. Murdaca, and A. Papa, Brodsky–Lepage–Mackenzie optimal renormalization scale setting for semihard processes, *Phys. Rev. D* 91, 114009 (2015)

16. S. Q. Wang, X. G. Wu, X. C. Zheng, G. Chen, and J. M. Shen, An analysis of $H \to \gamma\gamma$ up to three-loop QCD corrections, *J. Phys. G* 41, 075010 (2014)

17. S. Q. Wang, X. G. Wu, X. C. Zheng, J. M. Shen, and Q. L. Zhang, The Higgs boson inclusive decay channels $H \to b\bar{b}$ and $H \to gg$ up to four-loop level, *Eur. Phys. J. C* 74, 2825 (2014)

18. D. M. Zeng, S. Q. Wang, X. G. Wu, and J. M. Shen, The Higgs–Boson decay $H \to gg$ to order α_s^5 under the mMOM-scheme, arXiv: 1507.03222 [hep-ph]

19. S. Q. Wang, X. G. Wu, and S. J. Brodsky, Reanalysis of the higher order perturbative QCD corrections to hadronic Z decays using the principle of maximum conformality, *Phys. Rev. D* 90, 037503 (2014)

20. J. M. Shen, X. G. Wu, H. H. Ma, H. Y. Bi, and S. Q. Wang, Renormalization group improved pQCD prediction for $\Upsilon(1S)$ leptonic decay, *J. High Energy Phys.* 1506, 169 (2015)

21. S. J. Brodsky and X. G. Wu, Application of the principle of maximum conformality to the top-quark forward-backward asymmetry at the Tevatron, *Phys. Rev. D* 85, 114040 (2012)

22. S. Q. Wang, X. G. Wu, Z. G. Si, and S. J. Brodsky, Application of the principle of maximum conformality to the top-quark charge asymmetry at the LHC, *Phys. Rev. D* 90, 114034 (2014)

23. S. Q. Wang, X. G. Wu, Z. G. Si, and S. J. Brodsky, Predictions for the top-quark forward-backward asymmetry at high invariant pair mass using the principle of maximum conformality, arXiv: 1508.03739 [hep-ph]

24. C. F. Qiao, R. L. Zhu, X. G. Wu, and S. J. Brodsky, A possible solution to the B$\to \pi\pi$ puzzle using the principle of maximum conformality, *Phys. Lett. B* 748, 422 (2015) [arXiv: 1408.1158 [hep-ph]]

25. H. Baer, et al., The International Linear Collider Technical Design Report - Volume 2: Physics, arXiv: 1306.6352 [hep-ph]

26. J. P. Ma and Z. X. Zhang, The super *Z*-factory group, *Sci. China: Phys. Mech. Astron.* 53, 1947 (2010)

27. P. A. Baikov, K. G. Chetyrkin, J. H. Kuhn and J. Rittinger, Complete $\mathcal{O}(\alpha_s^4)$ QCD corrections to hadronic *Z*-decays, *Phys. Rev. Lett.* 108, 222003 (2012)

28. P. A. Baikov, K. G. Chetyrkin, and J. H. Kuhn, Order $\mathcal{O}(\alpha_s^4)$ QCD corrections to *Z* and tau decays, *Phys. Rev. Lett.* 101, 012002 (2008)

29. P. A. Baikov, K. G. Chetyrkin, and J. H. Kuhn, Adler function, Bjorken sum rule, and the Crewther relation to order $\mathcal{O}(\alpha_s^4)$ in a general gauge theory, *Phys. Rev. Lett.* 104, 132004 (2010)

30. P. A. Baikov, K. G. Chetyrkin, J. H. Kuhn, and J. Rittinger, Adler function, sum rules and Crewther relation of order $\mathcal{O}(\alpha_s^4)$: The singlet case, *Phys. Lett. B* 714, 62 (2012)

31. M. Czakon, P. Fiedler, and A. Mitov, Resolving the Tevatron top quark forward-backward asymmetry puzzle, *Phys. Rev. Lett.* 115, 052001 (2015)

32. M. Neubert, Scale setting in QCD and the momentum flow in Feynman diagrams, *Phys. Rev. D* 51, 5924 (1995)

33. M. Beneke and V. M. Braun, Naive non-Abelianization and resummation of fermion bubble chains, *Phys. Lett. B* 348, 513 (1995)

34. S. J. Brodsky, A. H. Hoang, J. H. Kuhn, and T. Teubner, Angular distributions of massive quarks and leptons close to threshold, *Phys. Lett. B* 359, 355 (1995)

35. H. Y. Bi, X. G. Wu, Y. Ma, H. H. Ma, S. J. Brodsky, and M. Mojaza, Degeneracy relations in QCD and the equivalence of two systematic all-orders methods for setting the renormalization scale, *Phys. Lett. B* 748, 13 (2015)

36. T. A. Aaltonen, et al. (CDF and D0 Collaborations), Combination of measurements of the top-quark pair production cross section from the Tevatron Collider, *Phys. Rev. D* 89, 072001 (2014)

37. S. J. Brodsky, G. F. de Teramond, H. G. Dosch, and J. Erlich, Light-front holographic QCD and emerging confinement, *Phys. Rep.* 584, 1 (2015)

38. V. M. Abazov, et al. (D0 Collaboration), Measurement of the forward-backward asymmetry in top quark-antiquark production in ppbar collisions using the lepton+jets channel, *Phys. Rev. D* 90, 072011 (2014)

39. V. M. Abazov, et al. (D0 Collaboration), Simultaneous measurement of forward-backward asymmetry and top polarization in dilepton final states from $t\bar{t}$ production at the Tevatron, arXiv: 1507.05666 [hep-ex]

40. T. Aaltonen, et al. (CDF Collaboration), Evidence for a mass dependent forward-backward asymmetry in top quark pair production, *Phys. Rev. D* 83, 112003 (2011)

41. T. Aaltonen, et al. (CDF Collaboration), Measurement of the top quark forward-backward production asymmetry and its dependence on event kinematic properties, *Phys. Rev. D* 87, 092002 (2013)

42. S. J. Brodsky and H. J. Lu, Commensurate scale relations in quantum chromodynamics, *Phys. Rev. D* 51, 3652 (1995)

43. A. H. Hoang, J. H. Kuhn, and T. Teubner, Radiation of light fermions in heavy fermion production, *Nucl. Phys. B* 452, 173 (1995)

Frontiers of Physics